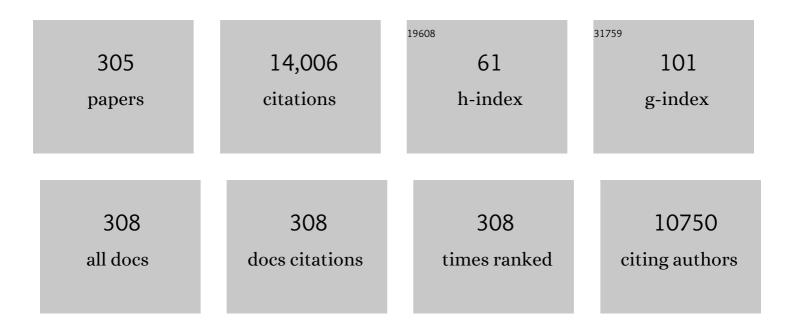
## Ming-Bo Yang

List of Publications by Year in descending order

Source: https://exaly.com/author-pdf/1413578/publications.pdf Version: 2024-02-01



#	Article	IF	CITATIONS
1	Progress on the morphological control of conductive network in conductive polymer composites and the use as electroactive multifunctional materials. Progress in Polymer Science, 2014, 39, 627-655.	11.8	553
2	Review on auxetic materials. Journal of Materials Science, 2004, 39, 3269-3279.	1.7	448
3	Hybrid graphene aerogels/phase change material composites: Thermal conductivity, shape-stabilization and light-to-thermal energy storage. Carbon, 2016, 100, 693-702.	5.4	351
4	Smart Ti <sub>3</sub> C <sub>2</sub> T <sub><i>x</i></sub> MXene Fabric with Fast Humidity Response and Joule Heating for Healthcare and Medical Therapy Applications. ACS Nano, 2020, 14, 8793-8805.	7.3	288
5	Stereocomplex Crystallite Network in Asymmetric PLLA/PDLA Blends: Formation, Structure, and Confining Effect on the Crystallization Rate of Homocrystallites. Macromolecules, 2014, 47, 1439-1448.	2.2	267
6	Largely enhanced thermal conductivity of poly (ethylene glycol)/boron nitride composite phase change materials for solar-thermal-electric energy conversion and storage with very low content of graphene nanoplatelets. Chemical Engineering Journal, 2017, 315, 481-490.	6.6	264
7	Hybrid network structure of boron nitride and graphene oxide in shape-stabilized composite phase change materials with enhanced thermal conductivity and light-to-electric energy conversion capability. Solar Energy Materials and Solar Cells, 2018, 174, 56-64.	3.0	223
8	An ice-templated assembly strategy to construct graphene oxide/boron nitride hybrid porous scaffolds in phase change materials with enhanced thermal conductivity and shape stability for light–thermal–electric energy conversion. Journal of Materials Chemistry A, 2016, 4, 18841-18851.	5.2	216
9	Flexible Anti-Biofouling MXene/Cellulose Fibrous Membrane for Sustainable Solar-Driven Water Purification. ACS Applied Materials & Interfaces, 2019, 11, 36589-36597.	4.0	216
10	Hybridizing graphene aerogel into three-dimensional graphene foam for high-performance composite phase change materials. Energy Storage Materials, 2018, 13, 88-95.	9.5	210
11	Macroporous three-dimensional MXene architectures for highly efficient solar steam generation. Journal of Materials Chemistry A, 2019, 7, 10446-10455.	5.2	208
12	Hierarchical graphene foam-based phase change materials with enhanced thermal conductivity and shape stability for efficient solar-to-thermal energy conversion and storage. Nano Research, 2017, 10, 802-813.	5.8	206
13	Self-assembled high-strength hydroxyapatite/graphene oxide/chitosan composite hydrogel for bone tissue engineering. Carbohydrate Polymers, 2017, 155, 507-515.	5.1	205
14	Enhanced comprehensive performance of polyethylene glycol based phase change material with hybrid graphene nanomaterials for thermal energy storage. Carbon, 2015, 88, 196-205.	5.4	189
15	High-performance composite phase change materials for energy conversion based on macroscopically three-dimensional structural materials. Materials Horizons, 2019, 6, 250-273.	6.4	187
16	Multilayer structured AgNW/WPU-MXene fiber strain sensors with ultrahigh sensitivity and a wide operating range for wearable monitoring and healthcare. Journal of Materials Chemistry A, 2019, 7, 15913-15923.	5.2	184
17	Polyethylene glycol based shape-stabilized phase change material for thermal energy storage with ultra-low content of graphene oxide. Solar Energy Materials and Solar Cells, 2014, 123, 171-177.	3.0	178
18	Self-assembled core-shell polydopamine@MXene with synergistic solar absorption capability for highly efficient solar-to-vapor generation. Nano Research, 2020, 13, 255-264.	5.8	174

#	Article	IF	CITATIONS
19	Boosting piezoelectric response of PVDF-TrFE via MXene for self-powered linear pressure sensor. Composites Science and Technology, 2021, 202, 108600.	3.8	165
20	Novel photodriven composite phase change materials with bioinspired modification of BN for solar-thermal energy conversion and storage. Journal of Materials Chemistry A, 2016, 4, 9625-9634.	5.2	163
21	All-weather-available, continuous steam generation based on the synergistic photo-thermal and electro-thermal conversion by MXene-based aerogels. Materials Horizons, 2020, 7, 855-865.	6.4	153
22	Stereocomplex formation of high-molecular-weight polylactide: A low temperature approach. Polymer, 2012, 53, 5449-5454.	1.8	150
23	Functionalized graphene oxide with ethylenediamine and 1,6-hexanediamine. New Carbon Materials, 2012, 27, 370-376.	2.9	131
24	Hierarchically interconnected porous scaffolds for phase change materials with improved thermal conductivity and efficient solar-to-electric energy conversion. Nanoscale, 2017, 9, 17704-17709.	2.8	131
25	Facile method to enhance output performance of bacterial cellulose nanofiber based triboelectric nanogenerator by controlling micro-nano structure and dielectric constant. Nano Energy, 2019, 62, 620-627.	8.2	122
26	Conductive thermoplastic vulcanizates (TPVs) based on polypropylene (PP)/ethylene-propylene-diene rubber (EPDM) blend: From strain sensor to highly stretchable conductor. Composites Science and Technology, 2016, 128, 176-184.	3.8	120
27	Enhanced Formation of Stereocomplex Crystallites of High Molecular Weight Poly( <scp>l</scp> -lactide)/Poly( <scp>d</scp> -lactide) Blends from Melt by Using Poly(ethylene) Tj ETQq1 1 0.	784 <b>31</b> 24 rgl	3T / <b>Qv</b> erlock
28	Multifunctional Thermal Management Materials with Excellent Heat Dissipation and Generation Capability for Future Electronics. ACS Applied Materials & Interfaces, 2019, 11, 18739-18745.	4.0	116
29	Self-Assembled Sponge-like Chitosan/Reduced Graphene Oxide/Montmorillonite Composite Hydrogels without Cross-Linking of Chitosan for Effective Cr(VI) Sorption. ACS Sustainable Chemistry and Engineering, 2017, 5, 1557-1566.	3.2	111
30	A bridge-arched and layer-structured hollow melamine foam/reduced graphene oxide composite with an enlarged evaporation area and superior thermal insulation for high-performance solar steam generation. Journal of Materials Chemistry A, 2020, 8, 2701-2711.	5.2	103
31	Induced Formation of Dominating Polar Phases of Poly(vinylidene fluoride): Positive Ion–CF <sub>2</sub> Dipole or Negative Ion–CH <sub>2</sub> Dipole Interaction. Journal of Physical Chemistry B, 2014, 118, 9104-9111.	1.2	102
32	Polyethylene glycol/graphene oxide aerogel shape-stabilized phase change materials for photo-to-thermal energy conversion and storage via tuning the oxidation degree of graphene oxide. Energy Conversion and Management, 2017, 146, 253-264.	4.4	99
33	Recent progress on chemical modification of cellulose for high mechanical-performance Poly(lactic) Tj ETQq1 1	0.784314	rgBT_/Overlo
34	Electrically insulating, layer structured SiR/GNPs/BN thermal management materials with enhanced thermal conductivity and breakdown voltage. Composites Science and Technology, 2018, 167, 456-462.	3.8	97
35	Flexible shape-stabilized phase change materials with passive radiative cooling capability for thermal management. Chemical Engineering Journal, 2021, 425, 131466.	6.6	97
36	Temperature induced gelation transition of a fumed silica/PEG shear thickening fluid. RSC Advances, 2015, 5, 18367-18374.	1.7	94

#	Article	IF	CITATIONS
37	Polymorphism of Racemic Poly( <scp>l</scp> -lactide)/Poly( <scp>d</scp> -lactide) Blend: Effect of Melt and Cold Crystallization. Journal of Physical Chemistry B, 2013, 117, 3667-3674.	1.2	93
38	A new approach to construct segregated structures in thermoplastic polyolefin elastomers towards improved conductive and mechanical properties. Journal of Materials Chemistry A, 2015, 3, 5482-5490.	5.2	91
39	Recent advances in polymer-based thermal interface materials for thermal management: A mini-review. Composites Communications, 2020, 22, 100528.	3.3	91
40	Photodriven Shape-Stabilized Phase Change Materials with Optimized Thermal Conductivity by Tailoring the Microstructure of Hierarchically Ordered Hybrid Porous Scaffolds. ACS Sustainable Chemistry and Engineering, 2018, 6, 6761-6770.	3.2	88
41	Bacterial cellulose/MXene hybrid aerogels for photodriven shape-stabilized composite phase change materials. Solar Energy Materials and Solar Cells, 2019, 203, 110174.	3.0	85
42	2D end-to-end carbon nanotube conductive networks in polymer nanocomposites: a conceptual design to dramatically enhance the sensitivities of strain sensors. Nanoscale, 2018, 10, 2191-2198.	2.8	83
43	A particular interfacial strategy in PVDF/OBC/MWCNT nanocomposites for high dielectric performance and electromagnetic interference shielding. Composites Part A: Applied Science and Manufacturing, 2018, 105, 118-125.	3.8	81
44	Electrically insulating POE/BN elastomeric composites with high through-plane thermal conductivity fabricated by two-roll milling and hot compression. Advanced Composites and Hybrid Materials, 2018, 1, 160-167.	9.9	81
45	Effect of temperature, crystallinity and molecular chain orientation on the thermal conductivity of polymers: a case study of PLLA. Journal of Materials Science, 2018, 53, 10543-10553.	1.7	79
46	Largely improved impact toughness of PA6/EPDM-g-MA/HDPE ternary blends: The role of core–shell particles formed in melt processing on preventing micro-crack propagation. Polymer, 2013, 54, 1938-1947.	1.8	78
47	Human Skin-Inspired Electronic Sensor Skin with Electromagnetic Interference Shielding for the Sensation and Protection of Wearable Electronics. ACS Applied Materials & Interfaces, 2018, 10, 40880-40889.	4.0	78
48	Highly sensitive and multifunctional piezoresistive sensor based on polyaniline foam for wearable Human-Activity monitoring. Composites Part A: Applied Science and Manufacturing, 2019, 121, 510-516.	3.8	78
49	A strain localization directed crack control strategy for designing MXene-based customizable sensitivity and sensing range strain sensors for full-range human motion monitoring. Nano Energy, 2020, 74, 104814.	8.2	77
50	A comparison of melt and solution mixing on the dispersion of carbon nanotubes in a poly(vinylidene) Tj ETQq	0 0 0 <sub>5.9</sub> BT /	Overlock 10 7
51	Recent Advances in Multiresponsive Flexible Sensors towards Eâ€skin: A Delicate Design for Versatile Sensing. Small, 2022, 18, e2103734.	5.2	76
52	A facile fabrication of shape memory polymer nanocomposites with fast light-response and self-healing performance. Composites Part A: Applied Science and Manufacturing, 2020, 135, 105931.	3.8	75
53	Boosting electrical and piezoresistive properties of polymer nanocomposites via hybrid carbon fillers: A review. Carbon, 2021, 173, 1020-1040.	5.4	71
	Towards balanced strength and toughness improvement of isotactic polypropylene papacomposites		

#	Article	IF	CITATIONS
55	Flexible TPU strain sensors with tunable sensitivity and stretchability by coupling AgNWs with rGO. Journal of Materials Chemistry C, 2020, 8, 4040-4048.	2.7	70
56	Hierarchical crystalline structure of HDPE molded by gas-assisted injection molding. Polymer, 2007, 48, 5486-5492.	1.8	67
57	Enhancing Thermomechanical Properties and Heat Distortion Resistance of Poly( <scp> </scp> -lactide) with High Crystallinity under High Cooling Rate. ACS Sustainable Chemistry and Engineering, 2015, 3, 654-661.	3.2	67
58	Low percolation threshold and balanced electrical and mechanical performances in polypropylene/carbon black composites with a continuous segregated structure. Composites Part B: Engineering, 2016, 99, 348-357.	5.9	67
59	Electro and Light-Active Actuators Based on Reversible Shape-Memory Polymer Composites with Segregated Conductive Networks. ACS Applied Materials & Interfaces, 2019, 11, 30332-30340.	4.0	66
60	Robust polymer-based paper-like thermal interface materials with a through-plane thermal conductivity over 9ÂWmâ^'1Kâ^'1. Chemical Engineering Journal, 2020, 392, 123784.	6.6	66
61	Multifunctional and highly sensitive piezoresistive sensing textile based on a hierarchical architecture. Composites Science and Technology, 2020, 197, 108255.	3.8	66
62	Facile fabrication of shape-stabilized polyethylene glycol/cellulose nanocrystal phase change materials based on thiol-ene click chemistry and solvent exchange. Chemical Engineering Journal, 2020, 396, 125206.	6.6	64
63	Influence of multiwall carbon nanotubes on the morphology, melting, crystallization and mechanical properties of polyamide 6/acrylonitrile–butadiene–styrene blends. Materials & Design, 2012, 34, 355-362.	5.1	62
64	Inorganic silica functionalized with PLLA chains via grafting methods to enhance the melt strength of PLLA/silica nanocomposites. Polymer, 2014, 55, 5760-5772.	1.8	61
65	Superior thermal interface materials for thermal management. Composites Communications, 2019, 12, 80-85.	3.3	61
66	Selective distribution and migration of carbon nanotubes enhanced electrical and mechanical performances in polyolefin elastomers. Polymer, 2017, 110, 1-11.	1.8	59
67	Nanofibrillar Poly(vinyl alcohol) Ionic Organohydrogels for Smart Contact Lens and Human-Interactive Sensing. ACS Applied Materials & Interfaces, 2020, 12, 23514-23522.	4.0	59
68	Morphology, rheology, crystallization behavior, and mechanical properties of poly(lactic) Tj ETQq0 0 0 rgBT /Over 2014, 131, .	lock 10 Tf 1.3	50 227 Td (a 57
69	Structuring tri-continuous structure multiphase composites with ultralow conductive percolation threshold and excellent electromagnetic shielding effectiveness using simple melt mixing. Polymer, 2016, 83, 34-39.	1.8	57
70	Light- and magnetic-responsive synergy controlled reconfiguration of polymer nanocomposites with shape memory assisted self-healing performance for soft robotics. Journal of Materials Chemistry C, 2021, 9, 5515-5527.	2.7	57
71	A Facile Route to Fabricate Highly Anisotropic Thermally Conductive Elastomeric POE/NG Composites for Thermal Management. Advanced Materials Interfaces, 2018, 5, 1700946.	1.9	56
72	Effect of temperature and strain rate on the tensile deformation of polyamide 6. Polymer, 2007, 48, 2958-2968.	1.8	55

#	Article	IF	CITATIONS
73	The enhanced nucleating ability of carbon nanotube-supported β-nucleating agent in isotactic polypropylene. Colloid and Polymer Science, 2010, 288, 681-688.	1.0	54
74	Redoxâ€Mediated Artificial Nonâ€Enzymatic Antioxidant MXene Nanoplatforms for Acute Kidney Injury Alleviation. Advanced Science, 2021, 8, e2101498.	5.6	54
75	Constructing a special â€~sosatie' structure to finely dispersing MWCNT for enhanced electrical conductivity, ultra-high dielectric performance and toughness of iPP/OBC/MWCNT nanocomposites. Composites Science and Technology, 2017, 139, 17-25.	3.8	51
76	Deformation-induced morphology evolution during uniaxial stretching of isotactic polypropylene: effect of temperature. Colloid and Polymer Science, 2012, 290, 261-274.	1.0	50
77	Deformation-induced structure evolution of oriented β-polypropylene during uniaxial stretching. Polymer, 2013, 54, 1259-1268.	1.8	50
78	Tuning the structure of graphene oxide and the properties of poly(vinyl alcohol)/graphene oxide nanocomposites by ultrasonication. Journal of Materials Chemistry A, 2013, 1, 3163.	5.2	49
79	Hierarchically Porous PVA Aerogel for Leakage-Proof Phase Change Materials with Superior Energy Storage Capacity. Energy & Fuels, 2020, 34, 2471-2479.	2.5	49
80	Crystalline morphology of β-nucleated controlled-rheology polypropylene. Polymer Testing, 2008, 27, 638-644.	2.3	48
81	Cylindritic structures of high-density polyethylene molded by multi-melt multi-injection molding. Polymer, 2011, 52, 3871-3878.	1.8	48
82	Multiple melting behaviour of annealed crystalline polymers. Polymer Testing, 2010, 29, 273-280.	2.3	47
83	Surface structure engineering for a bionic fiber-based sensor toward linear, tunable, and multifunctional sensing. Materials Horizons, 2020, 7, 2450-2459.	6.4	47
84	High-performance porous polylactide stereocomplex crystallite scaffolds prepared by solution blending and salt leaching. Materials Science and Engineering C, 2018, 90, 602-609.	3.8	46
85	Interfacial Radiation-Absorbing Hydrogel Film for Efficient Thermal Utilization on Solar Evaporator Surfaces. Nano Letters, 2021, 21, 10516-10524.	4.5	46
86	Dopamine-induced functionalization of cellulose nanocrystals with polyethylene glycol towards poly(L-lactic acid) bionanocomposites for green packaging. Carbohydrate Polymers, 2019, 203, 275-284.	5.1	45
87	Hierarchical unidirectional graphene aerogel/polyaniline composite for high performance supercapacitors. Journal of Power Sources, 2018, 397, 189-195.	4.0	44
88	Achieving improved electromagnetic interference shielding performance and balanced mechanical properties in polyketone nanocomposites via a composite MWCNTs carrier. Composites Part A: Applied Science and Manufacturing, 2020, 136, 105967.	3.8	43
89	Toughening of polyamide 6 with β-nucleated thermoplastic vulcanizates based on polypropylene/ethylene–propylene–diene rubber grafted with maleic anhydride blends. Materials & Design, 2012, 33, 104-110.	5.1	42
90	Electrical properties and morphology of carbon black filled PP/EPDM blends: effect of selective distribution of fillers induced by dynamic vulcanization. Journal of Materials Science, 2013, 48, 4942-4951.	1.7	42

#	Article	IF	CITATIONS
91	A high-performance temperature sensitive TPV/CB elastomeric composite with balanced electrical and mechanical properties via PF-induced dynamic vulcanization. Journal of Materials Chemistry A, 2014, 2, 16989-16996.	5.2	42
92	Suppression of phase coarsening in immiscible, co-continuous polymer blends under high temperature quiescent annealing. Soft Matter, 2014, 10, 3587.	1.2	42
93	Effects of Fe3O4 loading on the cycling performance of Fe3O4/rGO composite anode material for lithium ion batteries. Journal of Alloys and Compounds, 2016, 678, 80-86.	2.8	42
94	Exploring Nextâ€Generation Functional Organic Phase Change Composites. Advanced Functional Materials, 2022, 32, .	7.8	42
95	Low-entropy structured wearable film sensor with piezoresistive-piezoelectric hybrid effect for 3D mechanical signal screening. Nano Energy, 2021, 90, 106603.	8.2	41
96	Crystallization behavior of poly (vinylidene fluoride)/multi-walled carbon nanotubes nanocomposites. Journal of Materials Science, 2011, 46, 1542-1550.	1.7	40
97	Effects of annealing on structure and deformation mechanism of isotactic polypropylene film with rowâ€nucleated lamellar structure. Journal of Applied Polymer Science, 2013, 130, 1659-1666.	1.3	40
98	Greatly accelerated crystallization of poly(lactic acid): cooperative effect of stereocomplex crystallites and polyethylene glycol. Colloid and Polymer Science, 2014, 292, 163-172.	1.0	40
99	Effect of the core-forming polymer on phase morphology and mechanical properties of PA6/EPDM-g-MA/HDPE ternary blends. Polymer, 2015, 56, 395-405.	1.8	40
100	Flexible and Tough Cellulose Nanocrystal/Polycaprolactone Hybrid Aerogel Based on the Strategy of Macromolecule Cross-Linking via Click Chemistry. ACS Sustainable Chemistry and Engineering, 2019, 7, 15617-15627.	3.2	40
101	Morphologies of injection molded isotactic polypropylene/ultra high molecular weight polyethylene blends. Materials & Design, 2012, 35, 633-639.	5.1	39
102	Toughening of polypropylene with β-nucleated thermoplastic vulcanizates based on polypropylene/ethylene–propylene–diene rubber blends. Materials & Design, 2013, 51, 536-543.	5.1	39
103	High-melting-point crystals of poly( <scp>l</scp> -lactic acid) (PLLA): the most efficient nucleating agent to enhance the crystallization of PLLA. CrystEngComm, 2015, 17, 2310-2320.	1.3	39
104	High actuated performance MWCNT/Ecoflex dielectric elastomer actuators based on layer-by-layer structure. Composites Part A: Applied Science and Manufacturing, 2019, 125, 105527.	3.8	39
105	Phase change mediated mechanically transformative dynamic gel for intelligent control of versatile devices. Materials Horizons, 2021, 8, 1230-1241.	6.4	39
106	Grafting polymerization of polylactic acid on the surface of nanoâ€SiO <sub>2</sub> and properties of PLA/PLAâ€graftedâ€SiO <sub>2</sub> nanocomposites. Journal of Applied Polymer Science, 2013, 129, 3019-3027.	1.3	38
107	An extremely uniform dispersion of MWCNTs in olefin block copolymers significantly enhances electrical and mechanical performances. Polymer Chemistry, 2015, 6, 7160-7170.	1.9	38
108	Study on the melt flow behavior of glass bead filled polypropylene. Polymer Testing, 2005, 24, 490-497.	2.3	37

#	Article	IF	CITATIONS
109	Melt viscoelasticity, electrical conductivity, and crystallization of PVDF/MWCNT composites: Effect of the dispersion of MWCNTs. Journal of Applied Polymer Science, 2012, 125, E49.	1.3	37
110	Crystallization and reinforcement of poly (vinylidene fluoride) nanocomposites: Role of high molecular weight resin and carbon nanotubes. Polymer Testing, 2012, 31, 117-126.	2.3	37
111	Effect of the carbon black structure on the stability and efficiency of the conductive network in polyethylene composites. Journal of Applied Polymer Science, 2013, 129, 3382-3389.	1.3	37
112	Morphology, interfacial and mechanical properties of polylactide/poly(ethylene terephthalate glycol) blends compatibilized by polylactide-g-maleic anhydride. Materials & Design, 2014, 59, 524-531.	5.1	37
113	Poly(l-lactic acid)-polyethylene glycol-poly(l-lactic acid) triblock copolymer: A novel macromolecular plasticizer to enhance the crystallization of poly(l-lactic acid). European Polymer Journal, 2017, 97, 272-281.	2.6	37
114	Effect of temperature and time on the exfoliation and de-oxygenation of graphite oxide by thermal reduction. Journal of Materials Science, 2012, 47, 5097-5105.	1.7	36
115	Tailoring Crystalline Morphology by High-Efficiency Nucleating Fiber: Toward High-Performance Poly( <scp>l</scp> -lactide) Biocomposites. ACS Applied Materials & Interfaces, 2018, 10, 20044-20054.	4.0	36
116	Scalable Flexible Phase Change Materials with a Swollen Polymer Network Structure for Thermal Energy Storage. ACS Applied Materials & amp; Interfaces, 2021, 13, 59364-59372.	4.0	36
117	Effect of Melt and Mold Temperatures on the Solidification Behavior of HDPE during Gasâ€Assisted Injection Molding: An Enthalpy Transformation Approach. Macromolecular Materials and Engineering, 2009, 294, 336-344.	1.7	35
118	Effect of long chain branching on nonisothermal crystallization behavior of polyethylenes synthesized with constrained geometry catalyst. Polymer Engineering and Science, 2012, 52, 21-34.	1.5	35
119	Preparation of cellulose-graft-polylactic acid via melt copolycondensation for use in polylactic acid based composites: synthesis, characterization and properties. RSC Advances, 2016, 6, 1973-1983.	1.7	35
120	A rheological study on temperature dependent microstructural changes of fumed silica gels in dodecane. Soft Matter, 2012, 8, 10457.	1.2	34
121	Control of morphology and properties by the selective distribution of nano-silica particles with different surface characteristics in PA6/ABS blends. Journal of Materials Science, 2012, 47, 4620-4631.	1.7	34
122	Effect of nano-silica on the phase inversion behavior of immiscible PA6/ABS blends. Polymer Testing, 2013, 32, 141-149.	2.3	34
123	Toughening of PA6/EPDM-g-MAH/HDPE ternary blends via controlling EPDM-g-MAH grafting degree: the role of core–shell particle size and shell thickness. Polymer Bulletin, 2015, 72, 177-193.	1.7	34
124	Highly sensitive pressure sensor with broad linearity via constructing a hollow structure in polyaniline/polydimethylsiloxane composite. Composites Science and Technology, 2021, 201, 108546.	3.8	34
125	Flexible phase change hydrogels for mid-/low-temperature infrared stealth. Chemical Engineering Journal, 2022, 446, 137463.	6.6	34
126	Enhanced Thermal Conductivity and Balanced Mechanical Performance of PP/BN Composites with 1 vol% Finely Dispersed MWCNTs Assisted by OBC. Advanced Materials Interfaces, 2019, 6, 1900081.	1.9	33

#	Article	IF	CITATIONS
127	Effect of β-phase on the fracture behavior of dynamically vulcanized PP/EPDM blends studied by the essential work of fracture approach. European Polymer Journal, 2009, 45, 1448-1453.	2.6	32
128	Interfacial relaxation mechanisms in polymer nanocomposites through the rheological study on polymer/grafted nanoparticles. Polymer, 2016, 90, 264-275.	1.8	32
129	Scalable fabrication of flexible piezoresistive pressure sensors based on occluded microstructures for subtle pressure and force waveform detection. Journal of Materials Chemistry C, 2020, 8, 16774-16783.	2.7	32
130	A Waveâ€Driven Piezoelectric Solar Evaporator for Water Purification. Advanced Energy Materials, 2022, 12, .	10.2	32
131	Polymorphism of a high-molecular-weight racemic poly( <scp>l</scp> -lactide)/poly( <scp>d</scp> -lactide) blend: effect of melt blending with poly(methyl) Tj ETQq1	1 <b>0.7</b> 78431	4agBT /Ove
132	Tuning PVDF/PS/HDPE polymer blends to tri-continuous morphology by grafted copolymers as the compatibilizers. Polymer, 2018, 140, 188-197.	1.8	31
133	Aggregate of nanoparticles: rheological and mechanical properties. Nanoscale Research Letters, 2011, 6, 114.	3.1	30
134	Suppressing phase coarsening in immiscible polymer blends using nano-silica particles located at the interface. RSC Advances, 2015, 5, 74295-74303.	1.7	30
135	A Green and Facile Melt Approach for Hierarchically Porous Polylactide Monoliths Based on Stereocomplex Crystallite Network. ACS Sustainable Chemistry and Engineering, 2017, 5, 8334-8343.	3.2	30
136	Super-Toughed PLA Blown Film with Enhanced Gas Barrier Property Available for Packaging and Agricultural Applications. Materials, 2019, 12, 1663.	1.3	30
137	Double-layered and shape-stabilized phase change materials with enhanced thermal conduction and reversible thermochromism for solar thermoelectric power generation. Chemical Engineering Journal, 2022, 430, 132773.	6.6	30
138	Morphology of gas-assisted and conventional injection molded polycarbonate/polyethylene blend. Journal of Applied Polymer Science, 2006, 102, 3069-3077.	1.3	29
139	Induced formation of polar phases in poly(vinylidene fluoride) by cetyl trimethyl ammonium bromide. Journal of Materials Science, 2014, 49, 4171-4179.	1.7	29
140	Tailoring co-continuous like morphology in blends with highly asymmetric composition by MWCNTs: Towards biodegradable high-performance electrical conductive poly(l-lactide)/poly(3-hydroxybutyrate-co-4-hydroxybutyrate) blends. Composites Science and Technology, 2017, 152, 111-119.	3.8	29
141	Advanced Graphene@Sulfur composites via an in-situ reduction and wrapping strategy for high energy density lithium–sulfur batteries. Carbon, 2019, 150, 224-232.	5.4	29
142	Tailoring the impact behavior of polyamide 6 ternary blends via a hierarchical core–shell structure in situ formed in melt mixing. RSC Advances, 2015, 5, 14592-14602.	1.7	28
143	The effect of the grafted chains on the crystallization of PLLA/PLLA-grafted SiO2 nanocomposites. Colloid and Polymer Science, 2016, 294, 801-813.	1.0	28
144	Compatibilization of the poly(lactic acid)/poly(propylene carbonate) blends through <i>in situ</i> formation of poly(lactic acid)â€ <i>b</i> â€poly(propylene carbonate) copolymer. Journal of Applied Polymer Science, 2018, 135, 46009.	1.3	28

#	Article	IF	CITATIONS
145	Pore formation mechanism of oriented $\hat{I}^2$ polypropylene cast films during stretching and optimization of stretching methods: In-situ SAXS and WAXD studies. Polymer, 2019, 163, 86-95.	1.8	28
146	Large scale formation of various highly oriented structures in polyethylene/polycarbonate microfibril blends subjected to secondary melt flow. Polymer, 2014, 55, 6399-6408.	1.8	27
147	Oriented polypropylene cast films consisted of $\hat{l}^2$ -transcrystals induced by the nucleating agent self-assembly and its homogeneous membranes with high porosity. Polymer, 2018, 151, 136-144.	1.8	27
148	Formation and evolution of the carbon black network in polyethylene/carbon black composites: Rheology and conductivity properties. Journal of Applied Polymer Science, 2014, 131, .	1.3	26
149	Progress in polyketone materials: blends and composites. Polymer International, 2018, 67, 1478-1487.	1.6	26
150	Rational design of MnO2-nanosheets-decroated hierarchical porous carbon nanofiber frameworks as high-performance supercapacitor electrode materials. Electrochimica Acta, 2019, 324, 134891.	2.6	26
151	Mechanochemical preparation of thermoplastic cellulose oleate by ball milling. Green Chemistry, 2021, 23, 2069-2078.	4.6	26
152	Bismaleimide resin modified with diallyl bisphenol A and diallylp-phenyl diamine for resin transfer molding. Journal of Applied Polymer Science, 2001, 80, 2245-2250.	1.3	25
153	Highly thermally conductive electrospun stereocomplex polylactide fibrous film dip-coated with silver nanowires. Polymer, 2020, 194, 122390.	1.8	25
154	Dynamic Electrical and Rheological Percolation in Isotactic Poly(propylene)/Carbon Black Composites. Macromolecular Materials and Engineering, 2012, 297, 51-59.	1.7	24
155	Role of poly(lactic acid) in the phase transition of poly(vinylidene fluoride) under uniaxial stretching. Journal of Applied Polymer Science, 2013, 129, 1686-1696.	1.3	24
156	Effective dissolution of UHMWPE in HDPE improved by high temperature melting and subsequent shear. Polymer Engineering and Science, 2015, 55, 270-276.	1.5	24
157	Supercooling-dependent morphology evolution of an organic nucleating agent in poly( <scp>l</scp> -lactide)/poly( <scp>d</scp> -lactide) blends. CrystEngComm, 2017, 19, 1648-1657.	1.3	24
158	Carbon Nanotube Grafted Poly( <scp>l</scp> -lactide)-block-poly( <scp>d</scp> -lactide) and Its Stereocomplexation with Poly(lactide)s: The Nucleation Effect of Carbon Nanotubes. ACS Sustainable Chemistry and Engineering, 2016, 4, 2660-2669.	3.2	23
159	Effect of cross-linking degree of EPDM phase on the electrical properties and formation of dual networks of thermoplastic vulcanizate composites based on isotactic polypropylene (iPP)/ethylene–propylene–diene rubber (EPDM) blends. RSC Advances, 2016, 6, 74567-74574.	1.7	23
160	Role of carbon nanotube grafted poly(l-lactide)-block-poly(d-lactide) in the crystallization of poly(l-lactic acid)/poly(d-lactic acid) blends: Suppressed homocrystallization and enhanced stereocomplex crystallization. European Polymer Journal, 2016, 83, 42-52.	2.6	22
161	Formation of various crystalline structures in a polypropylene/polycarbonate in situ microfibrillar blend during the melt second flow. Physical Chemistry Chemical Physics, 2016, 18, 14030-14039.	1.3	22
162	Essential work of fracture evaluation of fracture behavior of glass bead filled linear low-density polyethylene. Journal of Applied Polymer Science, 2006, 99, 1781-1787.	1.3	21

#	Article	IF	CITATIONS
163	Balanced strength and ductility improvement of in situ crosslinked polylactide/poly(ethylene) Tj ETQq1 1 0.784	814 <sub>1</sub> , rg BT /	Overlock 10
164	Distinct positive temperature coefficient effect of polymer–carbon fiber composites evaluated in terms of polymer absorption on fiber surface. Physical Chemistry Chemical Physics, 2016, 18, 8081-8087.	1.3	21
165	Evolution of agglomerate structure of carbon nanotubes in multi-walled carbon nanotubes/polymer composite melt: A rheo-electrical study. Composites Part B: Engineering, 2012, 43, 3281-3287.	5.9	20
166	Role of gas delay time on the hierarchical crystalline structure and mechanical property of HDPE molded by gas-assisted injection molding. Colloid and Polymer Science, 2012, 290, 1133-1144.	1.0	20
167	Synergistic effect of stereocomplex crystals and shear flow on the crystallization rate of poly(l-lactic acid): A rheological study. RSC Advances, 2014, 4, 2733-2742.	1.7	20
168	Suppressing phase retraction and coalescence of co-continuous polymer blends: effect of nanoparticles and particle network. RSC Advances, 2014, 4, 49429-49441.	1.7	20
169	Effect of graphite oxide structure on the formation of stable self-assembled conductive reduced graphite oxide hydrogel. Journal of Materials Chemistry C, 2014, 2, 3846.	2.7	20
170	Insight into the formation of a continuous sheath structure for the PS phase in tri-continuous PVDF/PS/HDPE blends. RSC Advances, 2016, 6, 439-447.	1.7	20
171	Direct modification of polyketone resin for anion exchange membrane of alkaline fuel cells. Journal of Colloid and Interface Science, 2019, 556, 420-431.	5.0	20
172	Investigation on Tensile Deformation Behavior of Semi-Crystalline Polymers. Journal of Macromolecular Science - Physics, 2009, 48, 799-811.	0.4	19
173	Crystallization and fracture behaviors of highâ€density polyethylene/linear lowâ€density polyethylene blends: The influence of shortâ€chain branching. Journal of Applied Polymer Science, 2013, 129, 2103-2111.	1.3	19
174	Unusual hierarchical structures of mini-injection molded isotactic polypropylene/ultrahigh molecular weight polyethylene blends. European Polymer Journal, 2013, 49, 538-548.	2.6	19
175	Enantiomeric poly( <scp>d</scp> -lactide) with a higher melting point served as a significant nucleating agent for poly( <scp>l</scp> -lactide). CrystEngComm, 2015, 17, 4334-4342.	1.3	19
176	Effect of chain entanglement on the melt-crystallization behavior of poly(l-lactide) acid. Journal of Polymer Research, 2016, 23, 1.	1.2	19
177	Self-assembled nano-leaf/vein bionic structure of TiO <sub>2</sub> /MoS <sub>2</sub> composites for photoelectric sensors. Nanoscale, 2017, 9, 18194-18201.	2.8	19
178	Leakage-Proof and Malleable Polyethylene Wax Vitrimer Phase Change Materials for Thermal Interface Management. ACS Applied Energy Materials, 2021, 4, 11173-11182.	2.5	19
179	Self-Sensing Actuators Based on a Stiffness Variable Reversible Shape Memory Polymer Enabled by a Phase Change Material. ACS Applied Materials & Interfaces, 2022, 14, 22521-22530.	4.0	19
180	Enhancement effect of filler network on isotactic polypropylene/carbon black composite melts. Colloid and Polymer Science, 2011, 289, 1673-1681.	1.0	18

#	Article	IF	CITATIONS
181	Effect of annealing temperature on the mechanical properties, thermal behavior and morphology of β-iPP/PA6 blends. Materials & Design, 2012, 40, 392-399.	5.1	18
182	Effect of phase coarsening under melt annealing on the electrical performance of polymer composites with a double percolation structure. Physical Chemistry Chemical Physics, 2018, 20, 137-147.	1.3	18
183	Electrospun Modified Polyketone-Based Anion Exchange Membranes with High Ionic Conductivity and Robust Mechanical Properties. ACS Applied Energy Materials, 2021, 4, 5187-5200.	2.5	18
184	Interfacial interaction of polyvinylidene fluoride/multiwalled carbon nanotubes nanocomposites: A rheological study. Journal of Applied Polymer Science, 2011, 121, 3041-3046.	1.3	17
185	Characterization of PP/EPDM/HDPE Ternary Blends: The Role of Two EPDM with Different Viscosity and Processing Method. Polymer-Plastics Technology and Engineering, 2012, 51, 983-990.	1.9	17
186	MWCNTs Supported N,N′-Dicyclohexyl-1,5-diamino-2,6-naphthalenedicarboxamide: A Novel β-Nucleating Agent for Polypropylene. Journal of Macromolecular Science - Physics, 2012, 51, 2412-2427.	0.4	17
187	Nanoscale Morphology, Interfacial Hydrogen Bonding, Confined Crystallization and Greatly Improved Toughness of Polyamide 12/Polyketone Blends. Nanomaterials, 2018, 8, 932.	1.9	17
188	Driven by electricity: multilayered GO-Fe3O4@PDA-PAM flake assembled micro flower-like anode for high-performance lithium ion batteries. Applied Surface Science, 2020, 499, 143934.	3.1	17
189	Double yielding in PA6/TPV–MAH blends: Effect of dispersed phase with different content, modulus. Polymer, 2007, 48, 7404-7413.	1.8	16
190	Effect of repetitive processing on the mechanical properties and fracture toughness of dynamically vulcanized iPP/EPDM blends. Journal of Applied Polymer Science, 2011, 120, 86-94.	1.3	16
191	Structure of fumed silica gels in dodecane: enhanced network by oscillatory shear. Colloid and Polymer Science, 2012, 290, 151-161.	1.0	16
192	Composition, Morphology and Properties of Poly(lactic acid) and Poly(butylene succinate) Copolymer System via Coupling Reaction. Journal of Macromolecular Science - Pure and Applied Chemistry, 2013, 50, 861-870.	1.2	16
193	Effect of the content of $\hat{l}^2$ form crystals on biaxially stretched polypropylene microporous membranes and the tuning of pore structures. Polymer, 2019, 175, 177-185.	1.8	16
194	Improved dielectric properties of polymer-based composites with carboxylic functionalized multiwalled carbon nanotubes. Journal of Thermoplastic Composite Materials, 2019, 32, 473-486.	2.6	16
195	Lightweight poly (vinylidene fluoride)/silver nanowires hybrid membrane with different conductive network structure for electromagnetic interference shielding. Polymer Composites, 2021, 42, 522-531.	2.3	16
196	Study on Amino-functionalized Graphene Oxide/Poly(methyl methacrylate) Nanocomposites. Chemistry Letters, 2012, 41, 683-685.	0.7	15
197	Reinforcement and plasticization of PMMA grafted MWCNTs for PVDF composites. Composites Part B: Engineering, 2013, 53, 9-16.	5.9	15
198	Hierarchical crystalline structures and dynamic mechanical properties of injectionâ€molded bars of HDPE: attributes of temperature field. Polymers for Advanced Technologies, 2013, 24, 541-550.	1.6	15

Ming-Bo Yang

#	Article	IF	CITATIONS
199	Study of PE and iPP orientations on the surface of carbon nanotubes by using molecular dynamic simulations. Molecular Simulation, 2013, 39, 1013-1021.	0.9	15
200	Nanoparticle retarded shape relaxation of dispersed droplets in polymer blends: an understanding from the viewpoint of molecular movement. RSC Advances, 2014, 4, 41059-41068.	1.7	15
201	Enhancing crystallization rate and melt strength of <scp>PLLA</scp> with fourâ€arm <scp>PLLA</scp> grafted silica: The effect of molecular weight of the grafting <scp>PLLA</scp> chains. Journal of Applied Polymer Science, 2018, 135, 45675.	1.3	15
202	Tunable wrinkle structure formed on surface of polydimethylsiloxane microspheres. European Polymer Journal, 2018, 104, 99-105.	2.6	15
203	Effect of spatial confinement on the development of β phase of polypropylene. Polymer, 2009, 50, 4122-4127.	1.8	14
204	Structure and Properties of Radiation Cross-Linked Polypropylene Foam. Polymer-Plastics Technology and Engineering, 2011, 50, 1027-1034.	1.9	14
205	Co-crystallization of Blends of High-density Polyethylene with Linear Low-density Polyethylene: An Investigation with Successive Self-nucleation and Annealing (SSA) Technique. Journal of Macromolecular Science - Physics, 2013, 52, 1372-1387.	0.4	14
206	Synthesis of an Efficient Processing Modifier Silica- <i>g</i> -poly(lactic acid)/poly(propylene) Tj ETQq0 0 0 rgBT / Engineering Chemistry Research, 2017, 56, 14704-14715.	Overlock 1 1.8	0 Tf 50 467 - 14
207	Sulfaguanidine nanofiltration active layer towards anti-adhesive and antimicrobial attributes for desalination and dye removal. RSC Advances, 2019, 9, 20715-20727.	1.7	14
208	Stress-induced crystallization of biaxially oriented polypropylene. Journal of Applied Polymer Science, 2003, 89, 686-690.	1.3	13
209	Crystallization, rheological behavior and mechanical properties of poly(vinylidene fluoride) composites containing graphitic fillers: a comparative study. Polymer International, 2012, 61, 1031-1040.	1.6	13
210	The Complex Crystalline Structure of Polyethylene/Polycarbonate Microfibril Blends in a Secondary Flow Field. Macromolecular Chemistry and Physics, 2014, 215, 1146-1151.	1.1	13
211	A highly-deformable piezoresistive film composed of a network of carbon blacks and highly oriented lamellae of high-density polyethylene. RSC Advances, 2015, 5, 31074-31080.	1.7	13
212	Temperature: a nonnegligible factor for the formation of a structurally stable, self-assembled reduced graphite oxide hydrogel. RSC Advances, 2015, 5, 10-15.	1.7	13
213	Multi-functional carbon integrated rGO-Fe3O4@C composites as porous building blocks to construct anode with high cell capacity and high areal capacity for lithium ion batteries. Journal of Electroanalytical Chemistry, 2019, 840, 430-438.	1.9	13
214	Effects of modified nano-silica on the microstructure of PVDF and its microporous membranes. Journal of Polymer Research, 2019, 26, 1.	1.2	13
215	Boosting solar steam generation in dynamically tunable polymer porous architectures. Polymer, 2021, 226, 123811.	1.8	13
216	Essential work of fracture of glass bead filled low density polyethylene. Journal of Materials Science, 2005, 40, 5323-5326.	1.7	12

#	Article	IF	CITATIONS
217	Morphology evolution and the tri-continuous morphology formation of a PVDF/PS/HDPE ternary blend in melt mixing. RSC Advances, 2016, 6, 38803-38810.	1.7	12
218	Strong shear-driven large scale formation of hybrid shish-kebab in carbon nanofiber reinforced polyethylene composites during the melt second flow. Physical Chemistry Chemical Physics, 2016, 18, 30452-30461.	1.3	12
219	The effect of chain mobility on the coarsening process of co-continuous, immiscible polymer blends under quiescent melt annealing. Physical Chemistry Chemical Physics, 2017, 19, 12712-12719.	1.3	12
220	High-efficient crystallization promotion and melt reinforcement effect of diblock PDLA-b-PLLA copolymer on PLLA. Polymer, 2020, 186, 122021.	1.8	12
221	Improvement in the output performance of polyethylene oxide-based triboelectric nanogenerators by introducing core–shell Ag@SiO <sub>2</sub> particles. Journal of Materials Chemistry C, 2021, 10, 265-273.	2.7	12
222	Macromolecule Relaxation Directed 3D Nanofiber Architecture in Stretchable Fibrous Mats for Wearable Multifunctional Sensors. ACS Applied Materials & Interfaces, 2022, 14, 15678-15686.	4.0	12
223	A novel approach in preparing polymer/nano-CaCO3 composites. Frontiers of Chemical Engineering in China, 2008, 2, 115-122.	0.6	11
224	Effect of temperature gradient on the development of β phase polypropylene in dynamically vulcanized PP/EPDM blends. Colloid and Polymer Science, 2009, 287, 1237-1242.	1.0	11
225	Extension of the orientation region of high density polyethylene molded by gasâ€assisted injection molding: control of the thermal field. Polymer International, 2014, 63, 1997-2007.	1.6	11
226	Effect of the MWCNTs selective localization on the dielectric properties for PVDF/PS/HDPE ternary blends with in situ formed core–shell structure. RSC Advances, 2016, 6, 58493-58500.	1.7	11
227	A Facile Fabrication of PCL/OBC/MWCNTs Nanocomposite with Selective Dispersion of MWCNTs to Access Electrically Responsive Shape Memory Effect. Polymer Composites, 2019, 40, E1353-E1363.	2.3	11
228	Constructing Sandwich-Architectured Poly( <scp>l</scp> -lactide)/High-Melting-Point Poly( <scp>l</scp> -lactide) Nonwoven Fabrics: Toward Heat-Resistant Poly( <scp>l</scp> -lactide) Barrier Biocomposites with Full Biodegradability. ACS Applied Bio Materials, 2019, 2, 1357-1367.	2.3	11
229	Waterproof Phase Change Material with a Facilely Incorporated Cellulose Nanocrystal/Poly( <i>N</i> -isopropylacrylamide) Network for All-Weather Outdoor Thermal Energy Storage. ACS Applied Materials & Interfaces, 2020, 12, 53365-53375.	4.0	11
230	Biobinder Nanocoating for Upgrading the Assembling Structures of High-Capacity Composite Electrodes with a Robust Polymeric Artificial Solid Electrolyte Interphase. ACS Applied Materials & Interfaces, 2020, 12, 58201-58211.	4.0	11
231	Formation mechanism of hierarchically crystalline structures under coupled external fields in multi-melt multi-injection molding: Simulation and experiment. Composites Part B: Engineering, 2020, 188, 107770.	5.9	11
232	Imidazole-functionalized polyketone-based polyelectrolytes with efficient ionic channels and superwettability for alkaline polyelectrolyte fuel cells and multiple liquid purification. Journal of Materials Chemistry A, 2021, 9, 14827-14840.	5.2	11
233	In-situ construction of high-modulus nanospheres on elastomer fibers for linearity-tunable strain sensing. Chemical Engineering Journal, 2022, 431, 133488.	6.6	11
234	Effect of α―and βâ€nucleating agents on the fracture behavior of polypropyleneâ€ <i>co</i> â€ethylene. Journal of Applied Polymer Science, 2008, 108, 591-597.	1.3	10

#	Article	IF	CITATIONS
235	Dynamic Rheological Behavior of Copolymerized Linear Low-Density Polyethylenes: Effect of Molecular Weight and Its Distribution. Journal of Macromolecular Science - Physics, 2009, 48, 844-855.	0.4	10
236	Insight into the nucleating and reinforcing efficiencies of carbon nanofillers in poly(vinylidene) Tj ETQq0 0 0 rgB 2013, 48, 8509-8519.	[ /Overlocl 1.7	R 10 Tf 50 707 10
237	An unusual transition from point-like to fibrillar crystals in injection-molded polyethylene articles induced by lightly cross-linking and melt penetration. RSC Advances, 2015, 5, 21640-21650.	1.7	10
238	Formation of the three-dimensional (3D) interlinked hybrid shish-kebabs in injection-molded PE/PE-g-CNF composite by "structuring―processing. Composites Science and Technology, 2018, 157, 209-216.	3.8	10
239	Correlation between phase separation and rheological behavior in bitumen/SBS/PE blends. RSC Advances, 2018, 8, 41713-41721.	1.7	10
240	Mechanical Properties of Glass Bead-Filled Linear Low-Density Polyethylene. Journal of Elastomers and Plastics, 2004, 36, 251-265.	0.7	9
241	Effect of EPDM Content on Melt Flow, Microstructures and Fracture Behavior of Dynamically Vulcanized PP/EPDM Blends. Journal of Macromolecular Science - Physics, 2007, 46, 1127-1138.	0.4	9
242	Dynamic Rheological Behavior of Isotactic Polypropylene Filled With Nano-Calcium Carbonate Modified by Stearic Acid Coating. Journal of Macromolecular Science - Physics, 2009, 48, 329-343.	0.4	9
243	Photo-Driven Self-Healing of Arbitrary Nondestructive Damage in Polyethylene-Based Nanocomposites. ACS Applied Materials & Interfaces, 2020, 12, 1650-1657.	4.0	9
244	Synthesis of thermoplastic cellulose grafted polyurethane from regenerated cellulose. Cellulose, 2020, 27, 8667-8679.	2.4	9
245	Double yielding in PA6: Effect of mold temperature and moisture content. Journal of Polymer Science, Part B: Polymer Physics, 2007, 45, 1217-1225.	2.4	8
246	Effect of Injection Parameters and Addition of Nanoscale Materials on the Shrinkage of Polypropylene Copolymer. Journal of Macromolecular Science - Physics, 2009, 48, 573-586.	0.4	8
247	Mechanical and thermal characteristics and morphology of polyamide 6/isotactic polypropylene blends in the presence of a βâ€nucleating agent. Journal of Applied Polymer Science, 2011, 121, 554-562.	1.3	8
248	Effect of carbon nanotubeâ€supported β nucleating agent on the thermal properties, morphology, and mechanical properties of polyamide 6/isotactic polypropylene blends. Journal of Applied Polymer Science, 2012, 124, 993-999.	1.3	8
249	Crystallization kinetics of γ phase poly(vinylidene fluoride)(PVDF) induecd by tetrabutylammonium bisulfate. Journal of Polymer Research, 2014, 21, 1.	1.2	8
250	Morphological Evolution of Polystyrene/PolyÂethylene Blend Induced by Strong Second Melt Penetration. Macromolecular Materials and Engineering, 2016, 301, 714-724.	1.7	8
251	High Efficiency Conversion of Regenerated Cellulose Hydrogel Directly to Functionalized Cellulose Nanoparticles. Macromolecular Rapid Communications, 2017, 38, 1700409.	2.0	8
252	Enhanced performance of porous silicone-based dielectric elastomeric composites by low filler content of Ag@SiO <sub>2</sub> Core-Shell nanoparticles. Nanocomposites, 2018, 4, 238-243.	2.2	8

#	Article	IF	CITATIONS
253	Enhanced Rheological Properties of PLLA with a Purpose-Designed PDLA- <i>b</i> -PEG- <i>b</i> -PDLA Triblock Copolymer and the Application in the Film Blowing Process to Acquire Biodegradable PLLA Films. ACS Omega, 2019, 4, 13295-13302.	1.6	8
254	Scalable Synthesis of an Artificial Polydopamine Solidâ€Electrolyteâ€Interfaceâ€Assisted 3D rGO/Fe <sub>3</sub> O <sub>4</sub> @PDA Hydrogel for a Highly Stable Anode with Enhanced Lithiumâ€Ionâ€Storage Properties. ChemElectroChem, 2019, 6, 1069-1077.	1.7	8
255	Degradable ultrathin high-performance photocatalytic hydrogen generator from porous electrospun composite fiber membrane with enhanced light absorption ability. Journal of Materials Chemistry A, 2021, 9, 10277-10288.	5.2	8
256	Simulation and experimental studies on the formation and evolution of hierarchical crystalline structures at the multi-melt flow interface. Composites Part A: Applied Science and Manufacturing, 2021, 144, 106269.	3.8	8
257	Regenerated cellulose aerogel: Morphology control and the application as the template for functional cellulose nanoparticles. Journal of Applied Polymer Science, 2020, 137, 49127.	1.3	8
258	Transcrystallinity in a Polycarbonate(PC)/Polyethylene(PE) Blend Prepared by Gas-Assisted Injection Molding: A New Understanding of Its Formation Mechanism. Journal of Macromolecular Science - Physics, 2008, 47, 829-836.	0.4	7
259	Injection Molding Shrinkage and Mechanical Properties of Polypropylene Blends. Journal of Macromolecular Science - Physics, 2011, 50, 1747-1760.	0.4	7
260	A dynamic study on nonlinear viscoelastic behavior of isotactic polypropylene/carbon black composite melts. Colloid and Polymer Science, 2011, 289, 1927-1931.	1.0	7
261	A thermal method for quantitatively determinating the content of short chain branching in ethylene/α-olefin copolymers. Journal of Thermal Analysis and Calorimetry, 2012, 110, 1389-1394.	2.0	7
262	Influence of high molecular weight component on the hierarchical crystalline structures of injection-molded bars of polyethylene. Polymer International, 2014, 63, 1513-1522.	1.6	7
263	Contribution of residual solvent to the nucleation and reinforcement of poly (vinylidene fluoride). Polymer Testing, 2014, 34, 78-84.	2.3	7
264	New insights into the elasticity and multi-level relaxation of filler network with studies on the rheology of isotactic polypropylene/carbon black nanocomposite. RSC Advances, 2015, 5, 65874-65883.	1.7	7
265	Motion mode of poly(lactic acid) chains in film during strainâ€induced crystallization. Journal of Applied Polymer Science, 2016, 133, .	1.3	7
266	Unique crystallization behaviors of isotactic polypropylene in the presence of MWCNT supported β nucleating agent: Lower temperature T(αβ)-T(Ĩ²Ī±) interval and fast cooling preferred formation of β crystals. Polymer, 2016, 95, 26-35.	1.8	7
267	Diverse interfacial crystalline morphologies induced by poly (d-lactide) (PDLA) melt penetration process in multi-melt multi-injection molding (M3IM) system. Composites Part B: Engineering, 2018, 153, 429-436.	5.9	7
268	Synthesis of Inorganic Silica Grafted Three-arm PLLA and Their Behaviors for PLA Matrix. Chinese Journal of Polymer Science (English Edition), 2019, 37, 216-226.	2.0	7
269	Fabrication of poly(εâ€caprolactone) ( PCL) /poly(propylene carbonate) ( PPC) /ethyleneâ€Î±â€octene block copolymer ( OBC) triple shape memory blends with cycling performance by constructing a coâ€continuous phase morphology. Polymer International, 2020, 69, 702-711.	1.6	7
270	Tunable reversible deformation of semicrystalline polymer networks based on temperature memory effect. Polymer, 2021, 232, 124157.	1.8	7

#	Article	IF	CITATIONS
271	Double yielding in PA6/TPVâ€MAH blends: Effect of crosslinking degree of the dispersed phase. Journal of Polymer Science, Part B: Polymer Physics, 2009, 47, 912-922.	2.4	6
272	A new understanding concerning the influence of structural changes on the thermal behavior of cellulose. Journal of Polymer Research, 2015, 22, 1.	1.2	6
273	Influences of melt-draw ratio and annealing on the crystalline structure and orientation of poly(4-methyl-1-pentene) casting films. RSC Advances, 2016, 6, 62038-62044.	1.7	6
274	The massive formation of hybrid shishâ€kebab structures in <scp>HDPE</scp> / <scp>PA</scp> 6 microfibril blend subjected to melt second flow. Journal of Applied Polymer Science, 2017, 134, 45274.	1.3	6
275	Preparation of functionalized cellulose nanoparticles and their effect on the crystallization behaviors of poly( <scp>l</scp> ″actide) based nanocomposites. Polymer International, 2018, 67, 1535-1544.	1.6	6
276	Chemical-resistant polyamide 6/polyketone composites with gradient encapsulation structure: An insight into the formation mechanism. Polymer, 2021, 212, 123173.	1.8	6
277	A Facile and Rapid Approach to Lotusâ€5eedpodâ€5tructured Electronic Skin for Monitoring Diverse Physical Stimuli. Advanced Materials Technologies, 2021, 6, 2001084.	3.0	6
278	Combining â€~grafting to' and â€~grafting from' to synthesize comb-like NCC-g-PLA as a macromolecular modifying agent of PLA. Nanotechnology, 2021, 32, 385601.	1.3	6
279	Heterogeneous dispersion of the compatibilizer in the injection molding of polyamide 6/polypropylene blends. Journal of Applied Polymer Science, 2009, 113, 299-305.	1.3	5
280	Studies on the Blends of Polyamide66 and Thermoplastic Polyimide. Journal of Macromolecular Science - Physics, 2010, 49, 629-639.	0.4	5
281	Tailoring the crystalline morphologies and mechanical properties of highâ€density polyethylene parts by a change in the fluid flow pattern under gasâ€assisted injection molding. Journal of Applied Polymer Science, 2014, 131, .	1.3	5
282	Phase morphology control and the selective localization of MWCNT for suppressing dielectric loss and enhancing the dielectric constant of HDPE/PA11/MWCNT composites. RSC Advances, 2016, 6, 73056-73062.	1.7	5
283	Influence of HMW tail chains on the structural evolution of HDPE induced by second melt penetration. Physical Chemistry Chemical Physics, 2017, 19, 17745-17755.	1.3	5
284	Rapid, repeatable, highly sensitive and semi-quantitative colorimetric detection of elemental sulfur with a colored clathrate. Sensors and Actuators B: Chemical, 2019, 299, 126948.	4.0	5
285	Diameter dependence of hybrid shishâ€kebab structure in polyethylene/carbon material fiber composites. Journal of Polymer Science, Part B: Polymer Physics, 2019, 57, 297-303.	2.4	5
286	Highly anisotropic functional conductors fabricated by multi-melt multi-injection molding (M3IM): A synergetic role of multiple melt flows and confined interface. Composites Science and Technology, 2019, 171, 127-134.	3.8	5
287	Morphologies, interfacial interaction and mechanical performance of super-tough nanostructured PK/PA6 blends. Polymer Testing, 2020, 91, 106777.	2.3	5
288	A new insight into multi-tier structure tailoring: Synchronous utilization of particle migration and incompatible interface separation under shear flow. Polymer, 2020, 194, 122384.	1.8	4

#	Article	IF	CITATIONS
289	Effect of Spherical Nanoparticles on the Motion of Macromolecular Chains and Segments of Isotactic Polypropylene. I. Dynamic Mechanical and Thermal Properties. Journal of Macromolecular Science - Physics, 2010, 49, 870-885.	0.4	3
290	Enhancing the conductivity of isotactic polypropylene/polyethylene/carbon black composites by oscillatory shear. Colloid and Polymer Science, 2013, 291, 3005-3011.	1.0	3
291	Preparation and characterization of isotactic polypropylene/highâ€density polyethylene/carbon black conductive films with strainâ€sensing behavior. Journal of Applied Polymer Science, 2014, 131, .	1.3	3
292	Role of Controlled Diameter of Polyamide 6 (PA6) Fibers on the Formation of Interfacial Hybrid Crystal Morphology in HDPE/PA6 Microfibril Blend. Industrial & Engineering Chemistry Research, 2019, 58, 9056-9064.	1.8	3
293	Formation of nanosheets-assembled porous polymer microspheres via the combination effect of polymer crystallization and vapor-induced phase separation. Polymer, 2021, 231, 124118.	1.8	3
294	Hierarchical Distribution of β-Phase in Compression- and Injection-Molded, Polypropylene-Based TPV. Journal of Macromolecular Science - Physics, 2010, 50, 62-74.	0.4	2
295	Solvent-controlled formation of a reduced graphite oxide gel via hydrogen bonding. RSC Advances, 2016, 6, 27267-27271.	1.7	2
296	Excellent mechanical performance and enhanced dielectric properties of OBC/SiO2 elastomeric nanocomposites: effect of dispersion of the SiO2 nanoparticles. RSC Advances, 2017, 7, 46297-46305.	1.7	2
297	Piezoresistive behavior of elastomer composites with segregated network of carbon nanostructures and alumina. Nano Materials Science, 2023, 5, 312-318.	3.9	2
298	Effect of Nucleating Fillers on the Structure and Properties of Polypropylene Blends. Polymer-Plastics Technology and Engineering, 2012, 51, 998-1005.	1.9	1
299	Influence of Diameter on the Templated Crystallization of Polyethylene/Carbon Material Fiber Composites under Intense Shear Flow. ACS Omega, 2019, 4, 1060-1067.	1.6	1
300	Scalable and Heavy Foam Functionalization by Electrodeâ€Inspired Sticky Jammed Fluids for Efficient Inâ€Door Air Quality Management. Energy and Environmental Materials, 0, , .	7.3	1
301	Effects of convective schemes and geometric reconstruction scheme on interface of multiple melt flows. Polymer, 2022, 245, 124692.	1.8	1
302	Anomalous Melt Rheological Properties of Unimodal-MWD HDPE Blends. Polymer-Plastics Technology and Engineering, 2010, 49, 487-494.	1.9	0
303	Viscoelasticity Analysis of Spherical Nano-CaCO <sub>3</sub> -Filled Isotactic Polypropylene During a Uniaxial Tensile Test. Polymer-Plastics Technology and Engineering, 2010, 49, 1275-1283.	1.9	0
304	Characteristic Shear Rate for Nonlinear Viscoelastic Behavior in a Polydisperse Polymer Solution. Journal of Macromolecular Science - Physics, 2010, 50, 123-131.	0.4	0
305	Construction of "core–shell―structure for improved thermal conductivity and mechanical properties of polyamide 6 composites. Polymer Bulletin, 2021, 78, 2791-2803.	1.7	0